Heliyon 6 (2020) e03253

Contents lists available at ScienceDirect

Heliyon

journal homepage: www.cell.com/heliyon

Research article

Adsorption of the methyl green dye pollutant from aqueous solution using mesoporous materials MCM-41 in a fixed-bed column

Saja M. Alardhi, Talib M. Albayati *, Jamal M. Alrubaye

Department of Chemical Engineering, University of Technology, 52 Alsinaa St., PO Box 35010, Baghdad, Iraq

ARTICLE INFO

Keywords:
Chemical engineering
Environmental science
Industrial engineering
Environmental engineering
Waste treatment
Water treatment
Environmental chemical engineering
Separation
Fixed bed adsorption
Methyl green
MCM-41
Wastewater treatment

ABSTRACT

In this study, a Methyl Green (MG) dye pollutant was separated by Mobil Composition Matter No. 41 (MCM-41) in a fixed-bed continuous column with investigated three parameters, namely a bed height (2–6 cm), initial MG concentration (10–30 mgL^{-1}) and a process flow rate (0.8–1.6 mL min^{-1}). Results indicated that the highest bed capacity of 20.97 mg/g was obtained with respective to optimal values such as; 6 cm for a column height, 0.8 mL min^{-1} for flow rate, and an initial MG concentration 20 mgL^{-1}. Furthermore, a quantity of the adsorbed pollutant decreased as the flow rate increased, while increasing the initial MG concentration yielded the opposite effect. The column apparatus was performed properly at the low flow rate, whereas both the breakthrough and exhaustion time increased with the bed depth. Thomas and Yoon-Nelson models were applied for predicting the breakthrough curves and calculating the characteristic factors of the laboratory fixed-bed adsorption column, which were beneficial for process design. Based on regression coefficient analyses, results of employing the Yoon-Nelson model was found to be superior to the Thomas one. Breakthrough performance indicated that MCM-41 was suitable for applications in continuous adsorption regimes for MG dye. The mesoporous MCM-41 was recovered effectively by calcinations and employed again for four times in the continuous system successfully.

1. Introduction

Dye wastewater from the textile and dyestuff industries remains the most difficult wastewater to treat due to the intricate aromatic molecular structure of industrial dyes, which makes a challenging to biodegrade [1]. Even at low concentrations, dye pollutant concentrations can be extremely harmful to aquatic ecosystems [2]. The basic dyes (cationic dyes) are regarded as a highly problematic class of dyes with respect to the environment. Dyes commonly found in industrial effluents are mutagenic, allergenic, carcinogenic, toxic, and/or resistant to natural biological degradation [3]. Methyl green (MG) [$C_{27}H_{35}BrClN_3 \bullet ZnCl_2$] is a basic triphenylmethane-type dicationic dye that is widely utilized to change solution color in biology and medicine while serving as a photochromophore for exciting coagulated films [4]. The molecular structure of this dye is depicted in Figure 1.

Different dye elimination modes were developed to limit their impact in the environment, including ozonation, ion exchange, precipitation, coagulation-flocculation, microbial decomposition, photo-catalytic decolonization, sonochemical, filtration and membrane separation, liquid–liquid extraction, wet air oxidation, electrochemical methods and adsorption [5, 6]. However, adsorption is favored by the industrial processes due to its practicality and design simplicity, low cost, insensitivity to toxic materials, processing efficiency, and feasibility at very low concentrations [6, 7, 8]. Mesoporous materials with superior porous functionalities are provided by a uniform pore size, a wide surface area, and connectivity, have found many applications, such as in purification [9], catalysis [10, 11], drug delivery [12, 13, 14], humidity control [15, 16], heavy metals adsorption [17] and separation processes [18], but are also increasingly being used to treat the dyes found in wastewater effluents [19, 20, 21, 22, 23]. Batch investigations based on an adsorbent use were typically adopted to evaluate the adsorbate removal capacity and serve as a benchmark for determining the effectiveness for removing different adsorbates. In most industries, continuous fixed-bed adsorption columns were employed for dye-containing wastewater processing [24]. As this type of column acts in a dynamic state, the flow state (hydrodynamics) within the column exerts a significant influence on the downstream flow performance [25]. Empirical evidence indicates that columns are more applicable than batch-based designs because they ensure continuous flow over a fixed bed by increasing the capacity counter to the batch form of the treatment, where the gradient of

* Corresponding author.
E-mail addresses: talib_albyati@yahoo.com, 80046@uotechnology.edu.iq (T.M. Albayati).

https://doi.org/10.1016/j.heliyon.2020.e03253
Received 21 October 2019; Received in revised form 30 November 2019; Accepted 14 January 2020

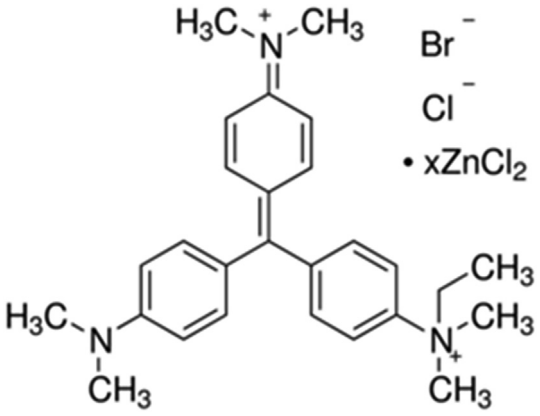

Figure 1. Molecular structure of methyl green.

concentration between the adsorbent and adsorbate declines over time [26]. Moreover, the results obtained from batch investigations are commonly not suitable for methods of the remediation since the contact time in the batch operation is not sufficiently long enough to achieve the equilibrium in continuous flow processes. Nevertheless, according to the literature, no studies have evaluated the removal of MG dye pollutants from the surface of MCM-41 in a fixed-bed column.

In this work, mesoporous silica MCM-41 was employed as an efficient adsorbent to remove MG dye pollutants from synthetic wastewater in a fixed-bed column for the first time. Furthermore, this study examines effects of the operational conditions such as a bed height, initial MG dye concentration and a flow rate on fixed-bed column dynamics. Kinetics models of the adsorption process in a fixed-bed column were performed using Thomas and Yoon approximations.

2. Materials and chemicals

2.1. Chemicals

MG ($C_{27}H_{35}BrClN_3$ •$ZnCl_2$), cetyltrimethyl ammonium bromide (CTAB, 99%), tetraethyl orthosilicate (TEOS, 98%), sodium hydroxide (NaOH), ethanol (EtOH, 99%) and citric acid ($C_6H_8O_7$) were purchased from Sigma Aldrich and used as received.

2.2. Preparation and characterization of MCM-41

The preparation procedure involves dissolving 0.34 g of sodium hydroxide and 1.01 g of cetyltrimethyl ammonium bromide in 30 mL distilled water. Then, the solution was left for 1 h with constant mixing at room temperature. Under static hydrothermal conditions, the prepared solution was blended for four days at 110 °C in a batch autocleaved reactor, The resulting material was filtered, washed with distilled water and ethanol, and left to dry in air at 25 °C [27]. Then, the powder was air-calcined at 823 K for 6 h in a furnace [Type: 1100 C 64 L, Origin: Italy] to remove the surfactant and template and then to obtain a white powder of MCM-41 [28]. Characterizations were also performed on the adsorbent in our previous study [22].

2.3. Adsorption of fixed-bed column

Fixed-bed column experiments were performed using a cylindrical tube (ID 0.7 cm and H 35 cm) made from glass as shown in Figure 2. The column was filled with different heights of MCM-41 and held in a position from below with glass wool. During the operation of the continuous adsorption, a blend consisting of MG was first compressed by pumping upward from a beaker through the top of the column using a peristaltic pump (type BT100-1F Hebei, China) while specimens were obtained from the bottom of the column at specific time intervals. The effect of

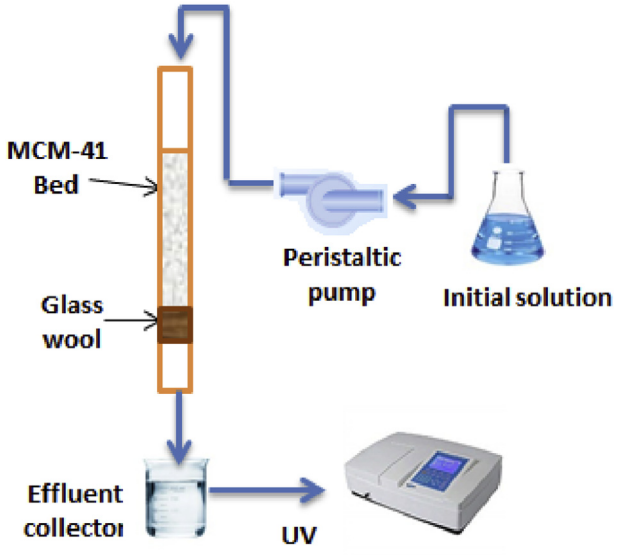

Figure 2. Setup of the flow sheet of the fixed-bed column.

different bed heights of 2, 4, and 6 cm, initial MG dye concentration of 10, 20, and 30 mg/L, and influent flow rates of 0.8, 1.2, and 1.6 mL/min on breakthrough curves (BTCs) were studied at a pH of 6 and 25 °C. The UV-Vis spectrophotometer (Type: U.V-1100, Origin: China) was employed for estimating the MG dye concentration in the outlet specimens at a consistent period while Thomas and Yoon models were employed for analyzing the BTCs and estimating constants.

2.4. Adsorption models in a fixed-bed column

The total percentage removal of the adsorbate can be determined from the ratio of the total mass of adsorbate (q_{total}) to the total quantity of the adsorbate that was compressed in the bed (m_{total}) [8].

$$\%\boldsymbol{R} = \frac{\boldsymbol{q_{total}}}{\boldsymbol{m_{total}}} \times 100 \quad (1)$$

The adsorbate uptake total mass (q_{total}, mg) was determined from:

$$q_{total} = \frac{Q \times Ci}{1000} \int_{t=0}^{t=t_{total}} \left(1 - \frac{C_e}{C_i}\right) dt \quad (2)$$

Where $\left(1 - \frac{C_e}{C_i}\right)$ represents the concentration of MG that adsorbed via MCM-41 (mgL^{-1}), C_i and C_e are the MG concentrations in the influent and effluent respectively, and Q represents the flow rate ($ml.min^{-1}$). The adsorbate total quantity (mg) that passed during the column was estimated from Eq. (3) [29]:

$$m_{total} = \frac{C_e \times t_e \times Q}{1000} \quad (3)$$

Where t_e is the time of exhaustion and the needed time to reach the exhaustion point within 1 min t_e is obtained, whereas the concentration of the MG solution in the effluent comes up with (95%) of the concentration at the inlet. The mass transfer zone (MTZ) length depends upon the adsorption rate and the flow rate of influent. The length of MTZ can be calculated as follow:

$$L_{MTZ} = L \frac{t_e - t_b}{t_e} \quad (4)$$

Where L is the height of the bed (cm), and t_b is the time (min) that is desired to reach the breakthrough point. The time of breakthrough t_b is computed, whereas the concentration of MG in the effluent feed $C_e$goes

beyond approximately 5% of the concentration of the influent solution C_i, which indicates that the time of the fixed-bed column is still valid.

The Thomas model is a highly general model used to predict the BTCs and explains the performance of the fixed-bed column. It is derived depending upon second-order kinetics and assumed that the sorption is not confined due to the chemical reaction, but instead, it is dominated via the mass transfer at the interface and the chemical reaction [30, 31]. The linearized representation of the Thomas model for the adsorption of the fixed bed is assigned in this equation [32]:

$$\ln\left(\frac{C_i}{C_e}-1\right)=\frac{K_{th}\,q_{th}\,m}{Q}-K_{th}C_i\,t \tag{5}$$

Where K_{th} is the rate constants for the Thomas model kinetic adsorption (mL.mg^{-1}. min^{-1}), $q_{th}$is the adsorption overall capacity calculated via the Thomas model (mg/g), where (t) is the time in (min). Thomas constants (K_{th} and q_{th}) are estimated employing nonlinear regression via drawing $\ln\left(\frac{C_i}{C_e}-1\right)$ against (t).

The Yoon-Nelson model is less complex, as it does not rely on an explanation of the data regarding the adsorbent nature, the adsorption physical factors bed, and adsorbate characteristics [33]. The linear formula is expressed as [34]:

$$\ln\left(\frac{C_e}{C_i\ -\ C_e}\right)=K_{yn}(t-\tau) \tag{6}$$

Where K_{yn} (min^{-1}) is the Yoon-Nelson model constant, and τ (min) is the desired time (min) to reach 50% adsorbate breakthrough. Using the intercept and linear drawing slope of $\ln\left(\frac{C_e}{C_i\ -\ C_e}\right)$ versus (t), K_{yn} and τ magnitudes can be calculated. To calculate the percentage error between the experimental and theoretical values, Eq. (7) was adopted.

$$\text{Percent Error}(\varepsilon)=\frac{[\text{experimental value}-\text{theoretical value}]}{\text{theoretical value}}\text{x}100\% \tag{7}$$

2.5. Regeneration of MCM-41

The processes involved in column regeneration were investigated beyond the tests of the adsorption were conducted at a 4 cm bed height, a 0.8 mL min^{-1} flow rate, and MG concentration of 20 mg. L^{-1}. When the experiments of adsorption were completed, the column bed had reached saturation. Thereafter, MCM-41 adsorbent was disintegrated for regenerating via shaking in 0.1 M NaOH solution, followed by centrifugation, washing, and drying at (70 °C), and reutilized again in the adsorption test (i.e., four cycles).

3. Results and discussions

3.1. Effect of fixed bed height

The breakthrough curves were acquired from the adsorption of the MG dye upon MCM-41 at different heights of bed heights (2, 4 and 6 cm) with an initial MG concentration of 20 mg/L of dye and a 0.8 ml/min flow rate, as presented in Figure 3. It is noticed that the time to reach breakthrough rose as the height of bed increased, the percentage of the dye removal increased from 41.17 to 49.57% if the height of bed was increased from 2 to 6 cm, this behavior was confirmed by [29]. The BTC shape noted for the 2 cm height of the bed was more upright than that for bed heights of 4 and 6 cm due to the shorter MTZ mass transfer region formed in the column. If the bed height was reduced, the adsorbent load in the column decreased, thus a smaller capacity of the bed for adsorbing the dye from the solution was the result, and the adsorption rate developed more quickly. Over time, the sorbent material became saturated and as a result, the dye concentration in the effluent solution increased [35].

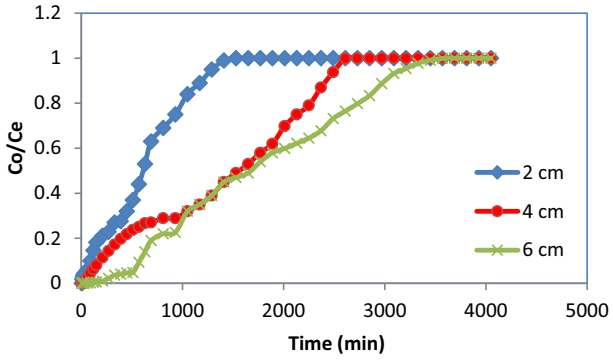

Figure 3. Breakthrough curves for adsorption of MG on MCM-41 beds at different heights (Co = 20 mg/L, Q = 0.8 mL/min, pH 6).

By increasing the height of the bed, a number of active sites which the dye was connected to were increased by expanding the surface area of the absorbent [36, 37]. The spread of the contaminant and a capacity of the sorbent material enhanced the dye removal by increasing the height of the bed, and thus, it was able to manage more quantities and volumes of wastewater and better removal efficiency. Such notice was promoted by other investigators [38, 39].

3.2. Initial concentration effect

In many cases, the process of diffusion depends on the concentration [40], so the initial dye concentration was determined to be more significant variable in the absorption process. Figure 4 depicts the influence of the initial concentration of the MG dye on the BTC at a fixed flow rate of 0.8 mL/min and a bed height of 4 cm. At the lower concentration, breakthrough curves were disbanded and occurred more slowly where the coefficient of the mass transfer was less due to the delaying phenomena of transport [41]. The gradient of concentration is the driving force for the operation of the mass transfer. Therefore, the higher initial dye concentration and high rates of the dye charging resulted in enhanced performance. The same kind of the behavior was obtained from [42].

The treated volume grew with the reduced concentration of the MG dye, and hence the BTCs shifted to the right [42]. If the concentration of the MG dye was greater, the BTC pattern approximately sloped more sharply, supplying a lower time of the breakthrough since the process of diffusion frequently relied upon the concentration. The elongated BTC was achieved by the reduced initial concentration of the MG dye due to the lower gradient of the concentration causing quieter transportation [43]. Accessible vacant sites of adsorbent were quickly packed at highly initial concentration of MG. Consequently, the time required for the breakthrough decreased.

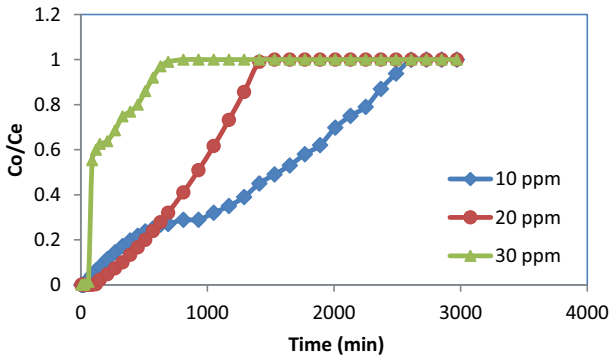

Figure 4. Breakthrough curves for adsorption of MG on MCM-41 beds at different dye concentrations (Q = 0.8 mL/min, L = 4 cm, pH 6).

3.3. Effect of initial flow rate

The effect of flow rate of MG dye adsorption on MCM-41 was examined by varying the flow rate (0.8, 1.2, and 1.6 ml/min), whereas the initial concentration of the MG dye and the height of the bed were held constant at 20 mg/L and 4 cm, correspondingly. Figure 5 depicts the relationship between the normalized concentration of the dye $\frac{Ce}{Ci}$ and time (min) at different flow rates. The speedy taking place of BTC was noted at greater flow rates due to, at the low rate of inlet dye solution, the fact that the MCM-41 has too much contact time with the dye that yielded a greater MG removal in the column [44]. As velocity developed, the MG dye eluted rapidly, and the rate of mass transfer increased, which increased the adsorption rate. Thus, the breakthrough times were achieved at higher rates of the flow [45].

The time of the breakthrough decreased from 1530 to 630 min when the rate of the flow increased from 0.8 to 1.6 mL/min as displayed in Table 1. The decrease in the solution residence time effects at low contact times between the adsorbent and solution. Therefore, equilibrium could not be attained while the lower flow rates cause ~~a~~ high residence time in the column [46].

3.4. Fixed-bed column dynamic modeling

3.4.1. Thomas model

The MG sorption per unit mass *qe* of MCM-41 and Thomas model rate constant (k_{Th}) were calculated by employing the data of adsorption. A linear regression, as displayed in Eq. (5), was applied to obtain the relevant constants. Figure 6 reveals the linear drawing between the $\left[\ln\left(\frac{Co}{Ce}\right)-1\right]$ and (t) at certain experimental circumstances (i.e., (a) bed height (2, 4, and 6 cm), (b) initial MG dye concentration (10, 20, and 30 mg/L), and (c) flow rates of influent (0.8, 1.2, and 1.6 mL/min)). From Table 2, the high value of the linear regression coefficient ($R^2 > 0.9$) demonstrated agreement that such a model fits properly with data of the experiments. In any event, the qe estimated magnitudes were near to those values of the experiment under different experimental conditions. In addition, it was noted from Table 2 that the lower (k_{Th}) value and the greater (qe) value were determined as the initial the MG dye concentration and bed height increased, the same results were obtained from [3, 47, 48], owing to the dye concentration gradient between the liquid phase and solid one, which behaved as a driving force for the adsorption. Consequently, the proper column performance required the greater initial concentration of the MG dye, which was determined to be the driving force. When the flow rate was increased, the (qe) magnitude vigorously declined, and (k_{Th}) increased. When the depth of the bed was increased, the (k_{Th}) decreased, but qe increased. Thus, the higher initial concentration of MG dye, the higher depth of the bed, and the lower flow were preferable for MG adsorption in the MCM-41 column [49, 50]. the percentage error between the experimental and theoretical values are shown in Table 2.

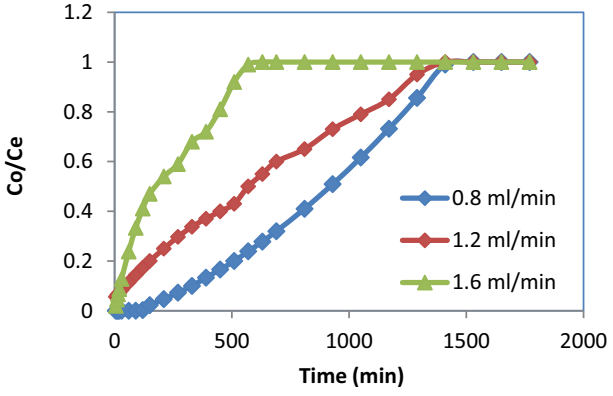

Figure 5. Breakthrough curves for adsorption of MG on MCM-41 beds at different flow rates (Co = 20 mg/L, L = 4 cm, pH 6).

Table 1. Parameters obtained from the breakthrough curves analysis.

L (cm) Q	Q (mL/min)	Ci (mg/L)	q_e (mg/g)	R%	C_e (mg/L)	L_{MTZ} (cm)
2	0.8	20	17.78	40.69	11.86	1.98
4	0.8	20	20.28	52.00	9.6	3.95
6	0.8	20	20. 49	52.94	9.4	5.89
4	0.8	30	14. 59	26.44	22.06	3.85
4	0.8	10	10.14	52	4.8	3.76
4	1.2	20	12.99	43.01	11.39	3.98
4	1.6	20	6.58	36.59	12.68	3.96

3.4.2. Yoon-Nelson model

The Yoon-Nelson model was utilized for investigating a behavior of the breakthrough of the MG dye with respect to MCM-41. A straight line

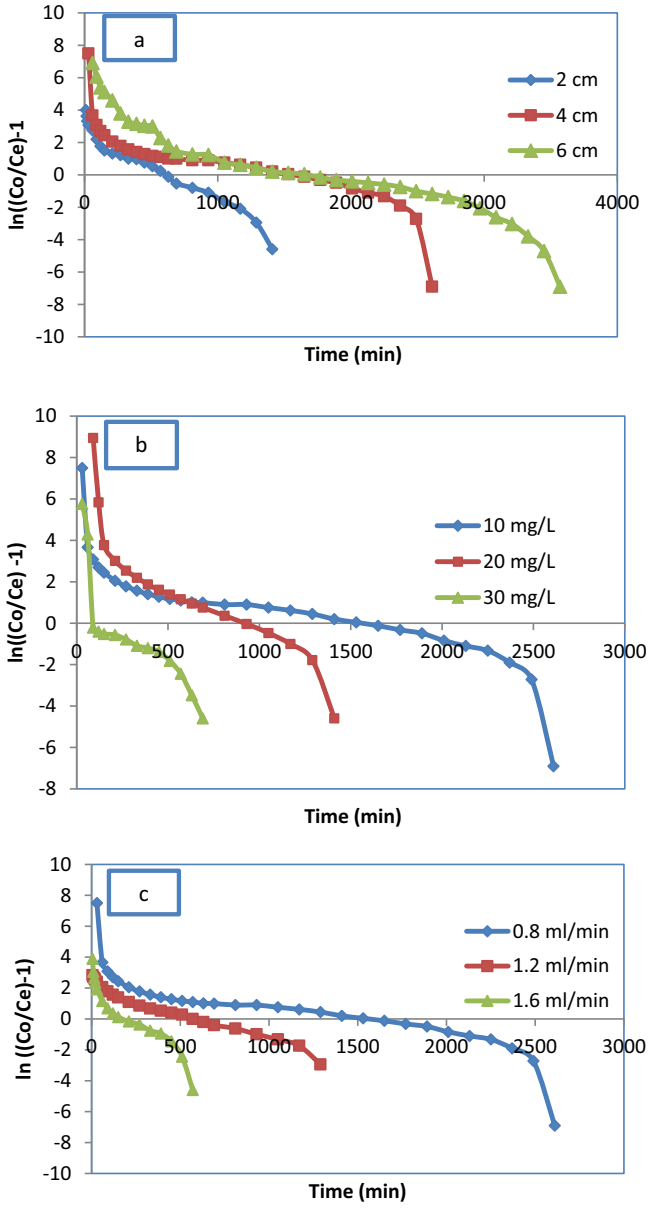

Figure 6. Linear plots of Thomas kinetic model for the adsorption of MG dye on MCM-41with (a) different bed height; (b) different initial concentration; (c) different flow rate.

Table 2. Thomas and Yoon parameters obtained for adsorption of MG on MCM-41 beds.

Column conditions			BTC analysis	Thomas model			ε	Yoon-Nelson model				ε
Q ml/min	L cm	Con. mg/l	q_{exp} mg/g	q_{Th} mg/g	K_{Th} ml/mg. min	R^2		q_y mg/g	K_{Yn} min^{-1}	τ min	R^2	
2	0.8	20	17.78	17.63	0.00024	94.95	0.85	17.63	0.0048	617	94.95	5.73
4	0.8	20	20.28	19.35	0.0002	72.8	4.80	19.18	0.0023	1342	74.85	2.28
6	0.8	20	20. 49	20.24	0.00012	89.36	1.23	20.97	0.002	1782	90.22	6.35
4	0.8	30	14. 59	20.00	0.00019	68.61	27.05	15.58	0.0101	260.8	68.61	4.86
4	0.8	10	10.14	9.67	0.00024	72.8	4.86	9.67	0.0024	1355	72.8	0.46
4	1.2	20	12.99	12.93	0.00021	95.98	0.46	12.93	0.0038	603.78	95.98	1.79
4	1.6	20	6.58	6.7	0.00053	88.83	1.79	6.7	0.0106	234. 69	88.83	0.85

was determined versus the drawing between the $\ln\left(\frac{Ce}{Co-Ce}\right)$ and(t), as depicted in Figure 7 under specific experimental conditions, namely (a) bed heights (2, 4, and 6 cm), (b) the initial MG dye concentrations (10, 20, and 30 mg/L), and (c) influent flow rates (0.8, 1.2, and 1.6 mL min^{-1}). It was noted that the greater (k_{YN}) magnitude was obtained when both the initial MG dye concentration and flow rate were higher, but the magnitude decreased with the greater bed height, and the same results were observed by [51]. In addition, the (τ) value decreased with an increase in the flow rate and initial concentration of the MG dye, but increased when the height of bed was increased due to the increase of the MG initial concentration increased the rivalry among the dye molecules for the adsorption location, which eventually yielded a greater rate of uptake [52].

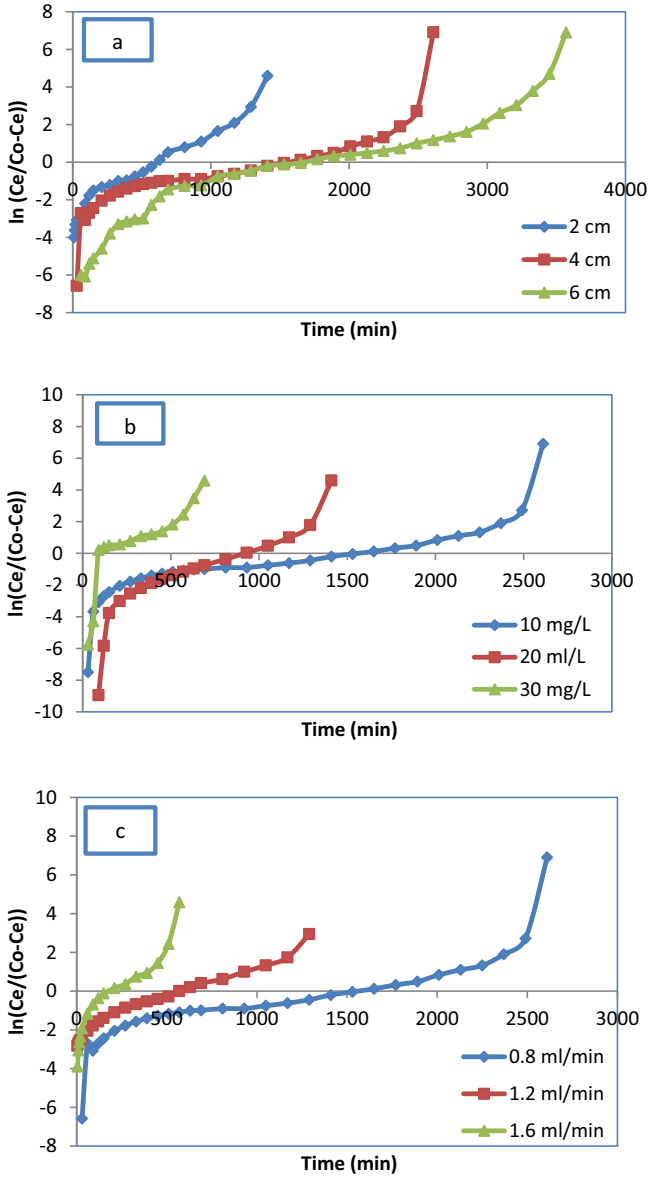

Figure 7. Linear plots of Yoon-Nelson kinetic model for the adsorption of MG dye on MCM-41 with (a) different bed height, (b) different initial concentration and (c) different flow rate.

3.5. MCM-41 fixed-bed regeneration

The explanation and results of the process are significant based on the ability to determine the number of times the adsorbent, which has the potential to greatly decreases the cost of the process and the capacity to restore the adsorbent. Table 3 and Figure 8 present the results. One can observe from such a figure that the time of breakthrough was decreased from 2730 to 1050 min, and the capacity of adsorption lowered beyond every cycle because of the active sites' gradual decomposition on the MCM-41 surface based on continuous operational conditions. In addition, one can recognize that the MG removal efficiency was reduced from 44% to 32% beyond four cycles (i.e., the experiment of regeneration possesses an attractive MCM-41 capability for reutilization since the

Table 3. Parameters obtained from the breakthrough curve analysis for adsorption of MG on regenerated MCM-41 beds.

Breakthrough parameters	Cycle 1	Cycle 2	Cycle 3	Cycle 4
qe (mg/g)	12.74	8.4	6.7	4.8
R%	44.38	33.24	36.82	32.00
Ce (mg/L)	11.12	13.35	12.63	13.6
LMTZ (cm)	3.96	3.97	3.98	3.98

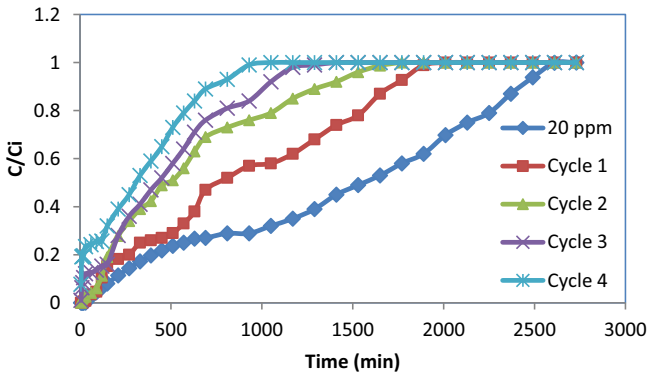

Figure 8. Breakthrough curves for adsorption of MG on regenerated MCM-41 beds at different cycles (L = 4cm, Co = 20 mg/L, pH 6).

Table 4. Comparison between this study and other studies.

No.	Method	Adsorbents	Adsorption capacity Q_{max} (mg g-1)	Reference
1	Batch adsorption	graphite oxide	29.42	[53]
2	Batch adsorption	graphene oxide	28.5	[54]
3	Batch adsorption	Bamboo	15.5	[19]
4	Fixed bed adsorption	Bamboo	–	[19]
5	Fixed bed adsorption	MCM-41	20.97	This study

medium reduction in the amplitude of adsorption was observed later in the subsequent cycles), but the removal percentage was not significantly altered.

3.6. Comparative study

This study deals with the investigation of MG removal from synthetic wastewater using MCM-41 in a fixed bed adsorption process because MCM-41 has a high surface area that reaches 1500 m^2/g compared to other adsorbents. Moreover, the process has the advantage to be applied for removing more MG in the actual industrial wastewater treatment due to its capability to adapt to many-sided processes, which can reduce processing and operational costs. A comparison between this study and others was presented in Table 4 and shown that MCM-41 is a promising adsorbent to remove the MG dye at the first time in the fixed-bed column system with the maximum capacity of the MCM-41 adsorption for the MG dye was 20.97 mg/g.

4. Conclusions

In an uninterrupted experiment, if the bed height was increased from 2 to 6 cm, the removal percentage and time to reach breakthrough increased, and the higher capacity of adsorption was achieved at the height of 6 cm. The reduction in flow rate from 1.6 to 0.8 mL/min resulted in an increase in the time to reach the breakthrough, and it was reduced by increasing the MG solution concentration at the inlet. The experimental data confirmed an acceptable fit to the mathematic Yoon-Nelson model of adsorption. Consequently, such a model can be utilized to evaluate the MG adsorption behavior in the continuous fixed-bed column system utilizing MCM-41. Regeneration experiments after four cycles discovered the unique MCM-41 potential for reutilization, since the scanty decrease in the amplitude of adsorption was identified in subsequent cycles.

Declarations

Author contribution statement

Saja M. Alardhi: Conceived and designed the experiments; Analyzed and interpreted the data.

Talib M. Albayati: Contributed reagents, materials, analysis tools or data; Wrote the paper.

Jamal M. Alrubaye: Performed the experiments.

Funding statement

This research did not receive any specific grant from funding agencies in the public, commercial, or not-for-profit sectors.

Competing interest statement

The authors declare no conflict of interest.

Additional information

No additional information is available for this paper.

Acknowledgements

I thank the Department of Chemical Engineering, University of Technology, Baghdad, Iraq for their scientific help.

References

[1] T.M. Albayati, K.R. Kalash, Polycyclic aromatic hydrocarbons adsorption from wastewater using different types of prepared mesoporous materials MCM-41in batch and fixed bed column, Process Saf. Environ. Prot. 133 (2020) 124–136.
[2] T.M. Albayati, A.A. Sabri, R.A. Alazawi, Separation of methylene blue as pollutant of water by SBA-15 in a fixed-bed column, Arabian J. Sci. Eng. 41 (2016) 2409–2415.
[3] S. Afroze, T.K. Sen, H.M. Ang, Adsorption performance of continuous fixed bed column for the removal of methylene blue (MB) dye using Eucalyptus sheathiana bark biomass, Res. Chem. Intermed. 42 (2016) 2343–2364.
[4] A. Nezamzadeh-Ejhieh, Z. Shams-Ghahfarokhi, Photodegradation of methyl green by nickel-dimethylglyoxime/ZSM-5 zeolite as a heterogeneous catalyst, J. Chem. 2013 (2013) 11.
[5] D. Pathania, S. Sharma, P. Singh, Removal of methylene blue by adsorption onto activated carbon developed from Ficus carica bast, Arabian J. Chem. 10 (2017) S1445–S1451.
[6] M. Rafatullah, O. Sulaiman, R. Hashim, A. Ahmad, Adsorption of methylene blue on low-cost adsorbents: a review, J. Hazard Mater. 177 (2010) 70–80.
[7] H. Chen, Y. Wang, Preparation of MCM-41 with high thermal stability and complementary textural porosity, Ceram. Int. 28 (2002) 541–547.
[8] M.T. Yagub, T.K. Sen, S. Afroze, H.M. Ang, Fixed-bed dynamic column adsorption study of methylene blue (MB) onto pine cone, Desalin. Water Treat. 55 (2015) 1026–1039.
[9] T.M. Albayati, A.M. Doyle, Purification of aniline and nitrosubstituted aniline contaminants from aqueous solution using beta zeolite, Chem. Bulg. J. Sci. Educ 23 (2014) 105–114.
[10] K. Bachari, R.M. Guerroudj, M. Lamouchi, Catalytic behavior of gallium-containing mesoporous silicas, Arabian J. Chem. 10 (2017) S301–S305.
[11] T.M.N. Albayati, S.E. Wilkinson, A.A. Garforth, A.M. Doyle, Heterogeneous alkane reactions over nanoporous catalysts, Transp. Porous Media 104 (2014) 315–333.
[12] B. Chen, G. Quan, Z. Wang, J. Chen, L. Wu, Y. Xu, G. Li, C. Wu, Hollow mesoporous silicas as a drug solution delivery system for insoluble drugs, Powder Technol. 240 (2013) 48–53.
[13] K. Czarnobaj, M. Prokopowicz, K. Greber, Use of materials based on polymeric silica as bone-targeted drug delivery systems for metronidazole, Int. J. Mol. Sci. 20 (2019) 1311.
[14] T.M. Albayati, A.A.A. Jassam, Synthesis and characterization of mesoporous materials as a carrier and release of prednisolone in drug delivery system, J. Drug Deliv. Sci. Technol. 53 (2019) 101176.
[15] R. Qi, X. Lin, J. Dai, H. Zhao, S. Liu, T. Fei, T. Zhang, Humidity sensors based on MCM-41/polypyrrole hybrid film via in-situ polymerization, Sens. Actuators B Chem. 277 (2018) 584–590.
[16] S. Kunchakara, M. Dutt, A. Ratan, J. Shah, V. Singh, R.K. Kotnala, Synthesis and characterizations of highly ordered KCl–MCM–41 porous nanocomposites for impedimetric humidity sensing, J. Porous Mater. 26 (2019) 389–398.
[17] T.M. Albayati, A.A. Sabri, D.B. Abed, Adsorption of binary and multi heavy metals ions from aqueous solution by amine functionalized SBA-15 mesoporous adsorbent in a batch system, Desalin. Water Treat. 151 (2019) 315–321.
[18] A.L. Khan, C. Klaysom, A. Gahlaut, I.F. Vankelecom, Polysulfone acrylate membranes containing functionalized mesoporous MCM-41 for CO2 separation, J. Membr. Sci. 436 (2013) 145–153.
[19] Ahmed Adnan Atshan, Adsorption of methyl green dye onto bamboo in batch and continuous system, Iraqi J. Chem. Pet. Eng. 15 (2014) 65–72.
[20] T.A. Arica, E. Ayas, M.Y. Arica, Magnetic MCM-41 silica particles grafted with poly (glycidylmethacrylate) brush: modification and application for removal of direct dyes, Microporous Mesoporous Mater. 243 (2017) 164–175.
[21] C.-K. Lee, S.-S. Liu, L.-C. Juang, C.-C. Wang, K.-S. Lin, M.-D. Lyu, Application of MCM-41 for dyes removal from wastewater, J. Hazard Mater. 147 (2007) 997–1005.
[22] T.M. Albayati, G.M. Alwan, O.S. Mahdy, High performance methyl orange capture on magnetic nanoporous MCM-41 prepared by incipient wetness impregnation method, Korean J. Chem. Eng. 34 (2017) 259–265.
[23] M. Anbia, S.A. Hariri, Removal of methylene blue from aqueous solution using nanoporous SBA-3, Desalination 261 (2010) 61–66.
[24] J.-M. Chern, Y.-W. Chien, Adsorption of nitrophenol onto activated carbon: isotherms and breakthrough curves, Water Res. 36 (2002) 647–655.
[25] S. Singh, V.C. Srivastava, I.D. Mall, Fixed-bed study for adsorptive removal of furfural by activated carbon, Colloid. Surf. Physicochem. Eng. Asp. 332 (2009) 50–56.
[26] V.K. Gupta, Suhas, I. Tyagi, S. Agarwal, R. Singh, M. Chaudhary, A. Harit, S. Kushwaha, Column operation studies for the removal of dyes and phenols using a low cost adsorbent, Global J. Environ. Sci. Manag. 2 (2016) 1–10.

[27] T.M. Albayati, Application of nanoporous material MCM-41 in a membrane adsorption reactor (MAR) as a hybrid process for removal of methyl orange, Desalin. Water Treat. 151 (2019) 138–144.
[28] L. Chen, T. Horiuchi, T. Mori, K. Maeda, Postsynthesis hydrothermal restructuring of M41S mesoporous molecular sieves in water, J. Phys. Chem. B 103 (1999) 1216–1222.
[29] S. Chatterjee, S. Mondal, S. De, Design and scaling up of fixed bed adsorption columns for lead removal by treated laterite, J. Clean. Prod. 177 (2018) 760–774.
[30] M. Calero, F. Hernáinz, G. Blázquez, G. Tenorio, M.A. Martín-Lara, Study of Cr (III) biosorption in a fixed-bed column, J. Hazard Mater. 171 (2009) 886–893.
[31] H.C. Thomas, Heterogeneous ion exchange in a flowing system, J. Am. Chem. Soc. 66 (1944) 1664–1666.
[32] J. López-Cervantes, D.I. Sánchez-Machado, R.G. Sánchez-Duarte, M.A. Correa-Murrieta, Study of a fixed-bed column in the adsorption of an azo dye from an aqueous medium using a chitosan–glutaraldehyde biosorbent, Adsorpt. Sci. Technol. 36 (2017) 215–232.
[33] Y.H. Yoon, J.H. Nelson, Application of gas adsorption kinetics I. A theoretical model for respirator cartridge service life, Am. Ind. Hyg. Assoc. J. 45 (1984) 509–516.
[34] S. Charola, R. Yadav, P. Das, S. Maiti, Fixed-bed adsorption of Reactive Orange 84 dye onto activated carbon prepared from empty cotton flower agro-waste, Sustain. Environ. Res. 28 (2018) 298–308.
[35] B. Nowack, T.D. Bucheli, Occurrence, behavior and effects of nanoparticles in the environment, Environ. Pollut. 150 (2007) 5–22.
[36] M.A.E. de Franco, C.B. de Carvalho, M.M. Bonetto, R. de Pelegrini Soares, L.A. Féris, Diclofenac removal from water by adsorption using activated carbon in batch mode and fixed-bed column: isotherms, thermodynamic study and breakthrough curves modeling, J. Clean. Prod. 181 (2018) 145–154.
[37] M.A.E. de Franco, Removal of amoxicillin from water by adsorption onto activated carbon in batch process and fixed bed column: kinetics, isotherms, experimental design and breakthrough curves modelling, J. Clean. Prod. 161 (2017), 10-956-2017 v.2161.
[38] S. Sadaf, H.N. Bhatti, Evaluation of peanut husk as a novel, low cost biosorbent for the removal of Indosol Orange RSN dye from aqueous solutions: batch and fixed bed studies, Clean Technol. Environ. Policy 16 (2014) 527–544.
[39] R. Han, Y. Wang, X. Zhao, Y. Wang, F. Xie, J. Cheng, M. Tang, Adsorption of methylene blue by phoenix tree leaf powder in a fixed-bed column: experiments and prediction of breakthrough curves, Desalination 245 (2009) 284–297.
[40] X. Luo, Z. Deng, X. Lin, C. Zhang, Fixed-bed column study for Cu2+ removal from solution using expanding rice husk, J. Hazard Mater. 187 (2011) 182–189.
[41] C.M. Futalan, C.-C. Kan, M.L. Dalida, C. Pascua, M.-W. Wan, Fixed-bed column studies on the removal of copper using chitosan immobilized on bentonite, Carbohydr. Polym. 83 (2011) 697–704.
[42] J. Cruz-Olivares, C. Pérez-Alonso, C. Barrera-Díaz, F. Ureña-Nuñez, M.C. Chaparro-Mercado, B. Bilyeu, Modeling of lead (II) biosorption by residue of allspice in a fixed-bed column, Chem. Eng. J. 228 (2013) 21–27.
[43] A.M. El-Kamash, Evaluation of zeolite A for the sorptive removal of Cs+ and Sr2+ ions from aqueous solutions using batch and fixed bed column operations, J. Hazard Mater. 151 (2008) 432–445.
[44] S. Singha, U. Sarkar, Analysis of the dynamics of a packed column using semi-empirical models: case studies with the removal of hexavalent chromium from effluent wastewater, Korean J. Chem. Eng. 32 (2015) 20–29.
[45] T.K. Sen, S.P. Mahajan, K.C. Khilar, Colloid-Associated contaminant transport in porous media: 1. Experimental studies, AIChE J. 48 (2002) 2366–2374.
[46] R. Gouran-Orimi, B. Mirzayi, A. Nematollahzadeh, A. Tardast, Competitive adsorption of nitrate in fixed-bed column packed with bio-inspired polydopamine coated zeolite, J. Environ. Chem. Eng. 6 (2018) 2232–2240.
[47] M. El Alouani, S. Alehyen, M. El Achouri, M.h. Taibi, Adsorption of cationic dye onto fly ash-based geopolymer: batch and fixed bed column studies, MATEC Web Conf 149 (2018), 02088.
[48] V. Dulman, S.-M. Cucu-Man, I. Bunia, M. Dumitras, Batch and fixed bed column studies on removal of Orange G acid dye by a weak base functionalized polymer, Desalin. Water Treat. 57 (2016) 14708–14727.
[49] Z. Aksu, F. Gönen, Biosorption of phenol by immobilized activated sludge in a continuous packed bed: prediction of breakthrough curves, Process Biochem. 39 (2004) 599–613.
[50] I.A.W. Tan, A.L. Ahmad, B.H. Hameed, Adsorption of basic dye using activated carbon prepared from oil palm shell: batch and fixed bed studies, Desalination 225 (2008) 13–28.
[51] H.-Y. Shu, M.-C. Chang, J.-J. Liu, Cation resin fixed-bed column for the recovery of valuable THAM reagent from the wastewater, Process Saf. Environ. Prot. 104 (2016) 571–586.
[52] T.M. Albayati, K.R. Kalash, Polycyclic aromatic hydrocarbons adsorption from wastewater using different types of prepared mesoporous materials MCM-41in batch and fixed bed column, Process Saf. Environ. Prot. 133 (2020) 124–136.
[53] A.A. Farghali, M. Bahgat, W.M.A. El Rouby, M.H. Khedr, Preparation, decoration and characterization of graphene sheets for methyl green adsorption, J. Alloy. Comp. 555 (2013) 193–200.
[54] P. Sharma, B.K. Saikia, M.R. Das, Removal of methyl green dye molecule from aqueous system using reduced graphene oxide as an efficient adsorbent: kinetics, isotherm and thermodynamic parameters, Colloid. Surf. Physicochem. Eng. Asp. 457 (2014) 125–133.